Supporting Information

A multifunctional Cu@g-C_3N_4 interfacial coating with synergistic desolvation promotion and interfacial pH stabilization for aqueous zinc-ion batteries

Jicheng Yan,[a] Zhongti Sun,[b] Changwei Dai,[a] Jiaxu Wang,[a] Benhua Wang,[a] Wuzhu Sun,[a] Chao Li*[a] and Jingyu Sun*[c]*

a. Discipline and Technology Center for High Temperature Functional Ceramics, Shandong Key Laboratory of Functional-Structural Integrated Ceramics, School of Materials Science and Engineering, Shandong University of Technology, Zibo, 255000, China. Email: chaol@sdut.edu.cn
b. School of Materials Science and Engineering, Jiangsu University, Zhenjiang, 212013, Jiangsu, China. Email: ztsun@ujs.edu.cn
c. College of Energy, Soochow University, Suzhou 215006, China. Email: sunjy86@suda.edu.cn

Materials

Vanadium pentoxide (V_2O_5), zinc sulfate heptahydrate ($ZnSO_4 \cdot 7H_2O$), *N*-methyl-2-pyrrolidone (NMP), poly(vinylidene fluoride) (PVDF), and urea were purchased from Aladdin Reagent (Shanghai, China). Potassium chloride (KCl) was purchased from Macklin Biochemical (Shanghai, China). Glass fiber separators (GF/A) were purchased from Whatman. Hydrogen peroxide (H_2O_2, 30 wt%), ethanol (C_2H_5OH), and copper (II) chloride ($CuCl_2$) were purchased from Sinopharm Chemical Reagent (Shanghai, China). All reagents were used as received without further purification.

Synthesis of Cu@g-C_3N_4

10 g of urea was dissolved in 15 mL of deionized water, followed by the addition of 67 mg of $CuCl_2$. The mixture was stirred at 90 °C until complete water evaporation, and the resulting solid was dried at 60 °C under vacuum for 12 h. The dried powder was ground for 30 min to obtain a homogeneous mixture, which was subsequently calcined at 550 °C for 3 h under a heating rate of 5 °C min^{-1}.

Preparation of Cu@g-C_3N_4@Zn anodes

Cu@g-C_3N_4 and PVDF were dispersed in *N*-methyl-2-pyrrolidone (NMP) at a mass ratio of 9:1 to form a homogeneous slurry, which was then coated onto zinc foil using the doctor blade method. After drying at 80 °C under vacuum overnight, the Cu@g-C_3N_4@Zn electrodes were obtained.

Synthesis of KVOH

The KVOH cathode material was synthesized following a previously reported procedure. Briefly, 0.364 g of V_2O_5 was dissolved in 50 mL of deionized water with the addition of 2 mL of 30 wt% H_2O_2. Separately, 0.0745 g of KCl (molar ratio K:V = 1:4) was dissolved in 30 mL of deionized water. The two solutions were combined and stirred magnetically for 30 min, then transferred into a 100 mL Teflon-lined

stainless-steel autoclave and heated at 120 °C for 6 h. The resulting precipitate was collected by filtration, washed three times with deionized water and ethanol, and dried at 60 °C for 10 h, yielding a green powder.

Material characterization

Sample morphology was examined by scanning electron microscopy (SEM, FEI Quanta 250) and transmission electron microscopy (TEM, FEI Tecnai G2 F20 S-TWIN). Atomic-resolution imaging was performed using aberration-corrected high-angle annular dark-field scanning transmission electron microscopy (HAADF-STEM, Thermo Scientific Themis Z). X-ray powder diffraction (XRD) patterns were collected on a Bruker D8 Advance diffractometer using Cu Kα radiation. X-ray photoelectron spectroscopy (XPS) was performed on a Thermo Scientific ESCALAB 250Xi instrument. Cu loading was quantified by inductively coupled plasma optical emission spectrometry (ICP-OES, Thermo Fisher iCAP PRO).

Electrochemical measurements

All CR2032-type coin cells were assembled under ambient conditions using glass fiber (GF/A, Whatman) as the separator with 90 μL of electrolyte. The KVOH cathode was prepared by casting a slurry of active material, conductive carbon (Super P), and PVDF binder in a mass ratio of 7:2:1 onto carbon paper, followed by drying at 80 °C under vacuum for 12 h. The active material mass loading was approximately 1.2 mg cm^{-2}. Galvanostatic charge–discharge measurements were performed on a NEWARE battery testing system at 25 °C.

Electrochemical measurements including linear sweep voltammetry (LSV), cyclic voltammetry (CV), Tafel polarization, electrochemical impedance spectroscopy (EIS), and chronoamperometry (CA) were conducted on a CHI 660E electrochemical workstation. CV of Zn//Ti asymmetric cells were performed in the voltage range of −0.4 to 0.6 V at a scan rate of 1 mV s^{-1}, with Zn foil serving as both the counter and

reference electrode. For Zn//KVOH full cells, CV was recorded in the range of 0.2–1.6 V at 0.1 mV s^{-1}. CA curves were recorded at a constant overpotential of −150 mV for 800 s. EIS was performed over a frequency range of 0.01 Hz to 100 kHz with an AC amplitude of 10 mV. HER activity was evaluated by LSV in a three-electrode configuration, with Zn foil, Pt plate, and Ag/AgCl as the working, counter, and reference electrodes, respectively, over the potential range of −0.95 to −2.0 V vs. Ag/AgCl at a scan rate of 1 mV s^{-1}. Corrosion behavior was assessed by Tafel polarization in a three-electrode configuration, with Zn foil as the working and counter electrode, and Ag/AgCl as the reference electrodes in 2 M $ZnSO_4$ solution at 1 mV s^{-1}.

Theoretical calculations

All the calculations were performed by the spin-unrestricted density functional theory, executed by the Vienna Ab-initio Simulation Package with the projector augmented wave pseudopotential.[1] The electronic exchange-correlation interactions were treated by the GGA-PBE functional.[2] To accurately evaluate the interaction of Zn ion on the various substrates, the DFT-D3 correction schemed by the Grimme et al. was adopted.[3] The kinetic energy cutoff with the plane wave basis set was 400 eV. The integrated Brillouin zone was sampled by the mesh size of 3×3×1 and 5×5×1 for the geometric optimizations and static calculations, respectively. The total energy and residual force per atom were converged by the respective standard of 10^{-4} eV and 0.02 eV/Å. The uptake of Zn on Cu@g-C_3N_4, g-C_3N_4, and graphene surface was considered. Cu@g-C_3N_4 was marked by the Cu atom anchored into the graphitized g-C_3N_4 supercell with 2×2 size, compared with the bare g-C_3N_4 and bare-graphene with 5×5 supercell. The adsorption energy of Zn was calculated by the following formula:

$$E_{ads}=E_{total}-E_{surf}-E_{Zn}.$$

Where E_{total} and E_{surf} represent the total energy of substrates with and without Zn atom, respectively. E_{Zn} marks the atomic energy of Zn.

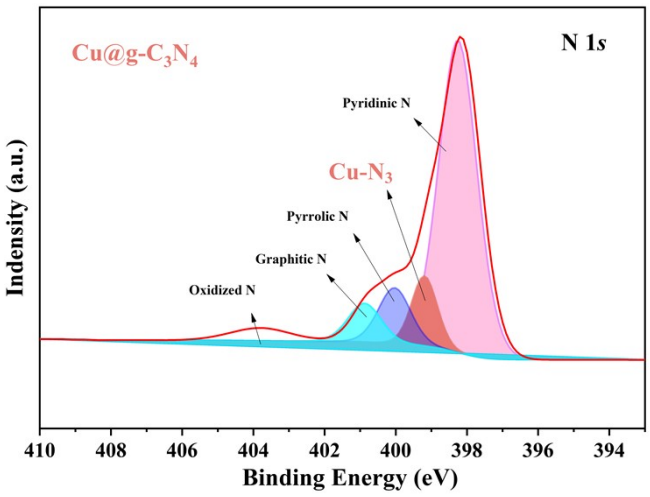

Fig. S1 High-resolution N 1*s* XPS spectrum of Cu@g-C_3N_4.

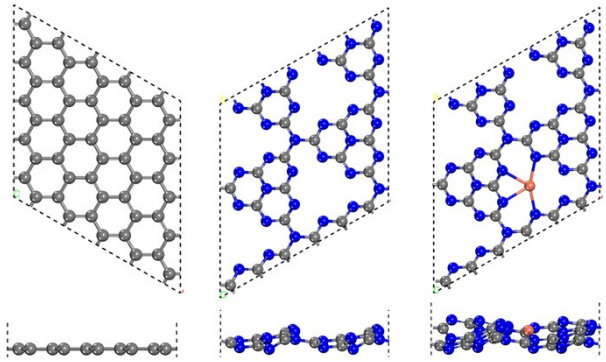

Fig. S2 Optimized structural models of graphene, pristine g-C_3N_4, and Cu@g-C_3N_4 used for DFT calculations (Cu, orange; N, blue; C, grey).

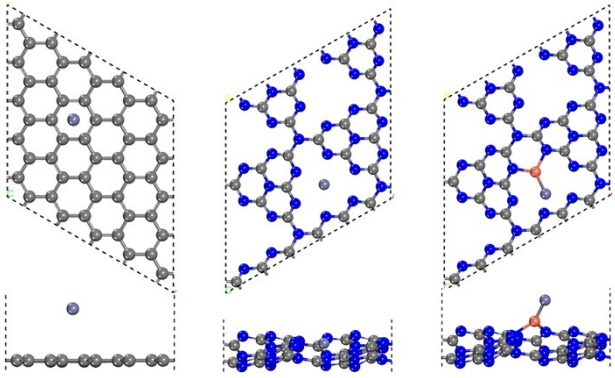

Fig. S3 Optimized adsorption configuration of Zn on the (a) graphene, (b) g-C_3N_4, (c) Cu@g-C_3N_4 substrate. The orange, brown, blue, and grey ball marks Cu, Zn, N and C atom, respectively.

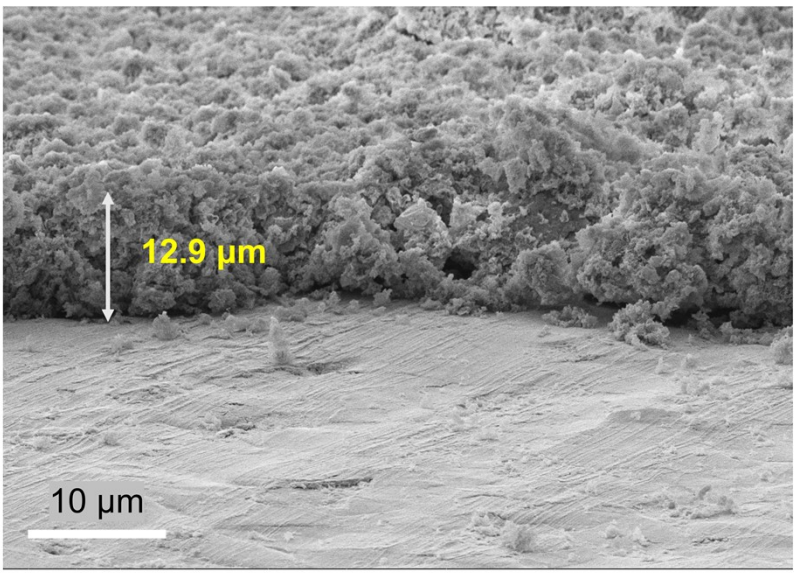

Fig. S4 Cross-sectional SEM image of the Cu@g-C_3N_4 coating on Zn foil.

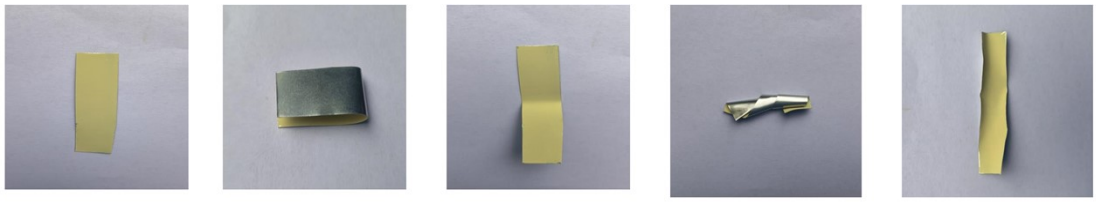

Fig. S5 Photographs of Cu@g-C_3N_4@Zn under bending and twisting tests, demonstrating the mechanical flexibility and interfacial adhesion of the coating.

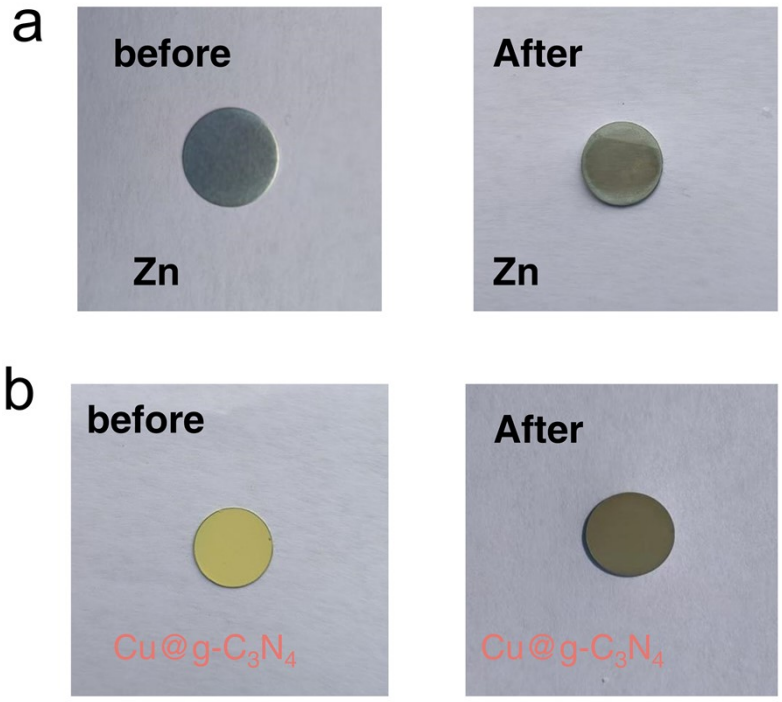

Fig. S6. Optical photographs of (a) bare Zn and (b) Cu@g-C_3N_4@Zn before and after immersion in 2 M $ZnSO_4$ for 7 days.

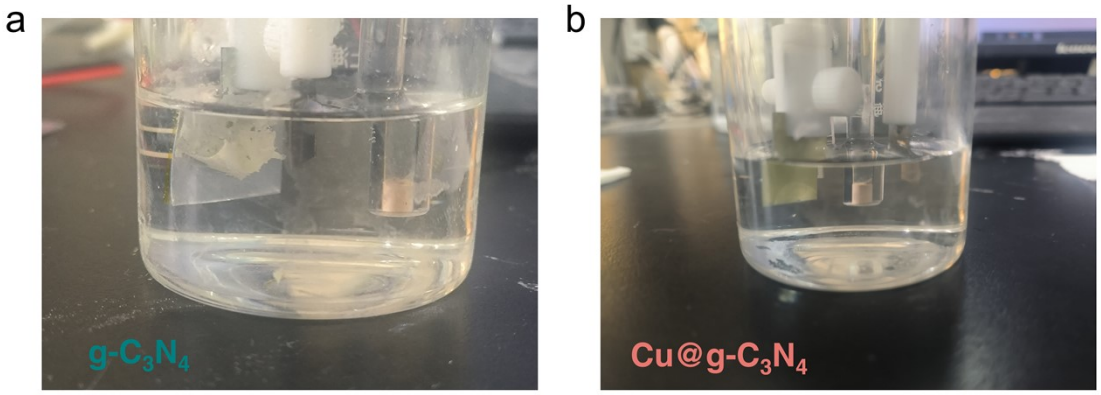

Fig. S7. Photographs of (a) g-C_3N_4@Zn and (b) Cu@g-C_3N_4@Zn electrodes after LSV testing, showing the improved structural integrity of the Cu@g-C_3N_4 coating.

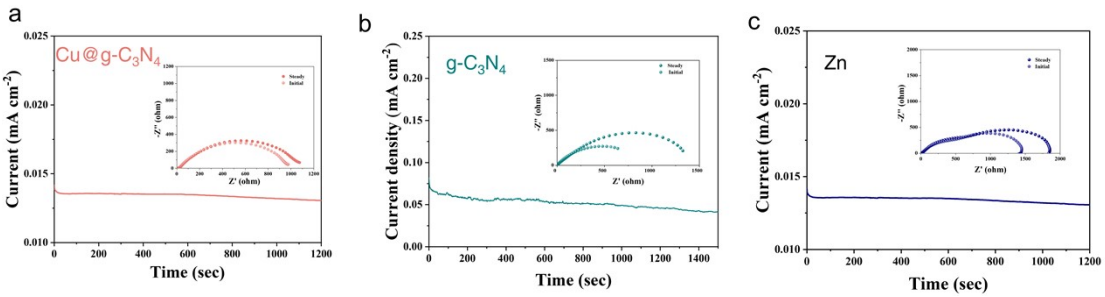

Fig. S8. Chronoamperometric current–time curves and Nyquist plots before and after polarization for Zn^{2+} transference number measurements of (a) Cu@g-C_3N_4@Zn, (b) g-C_3N_4@Zn, and (c) bare Zn symmetric cells.

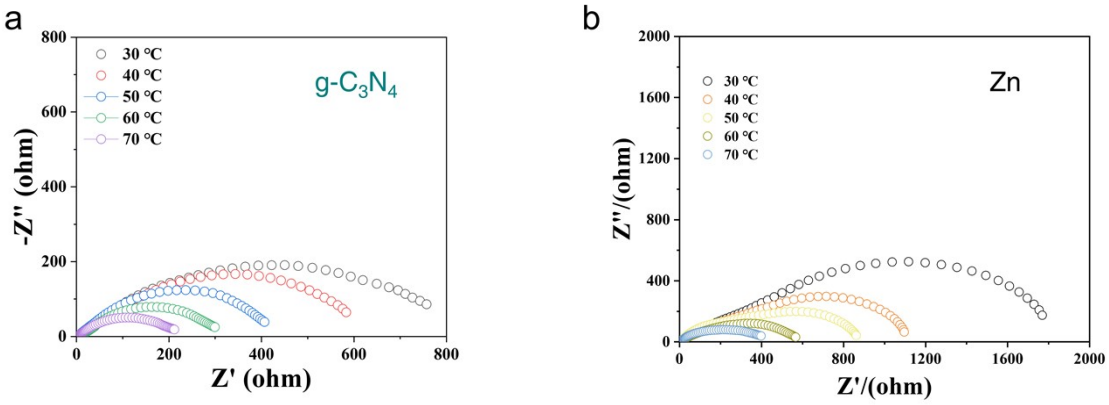

Fig. S9 Temperature-dependent EIS Nyquist plots of (a) g-C_3N_4@Zn and (b) bare Zn symmetric cells measured from 30 to 70 °C.

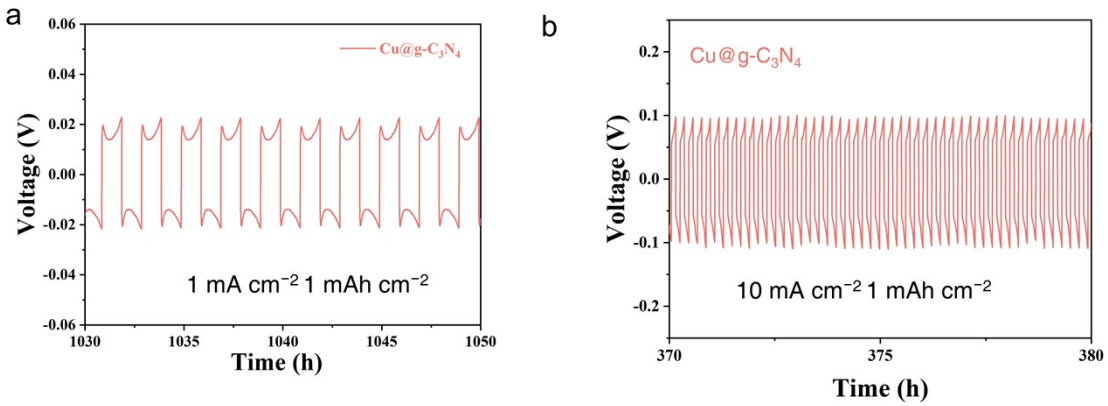

Fig. S10 Enlarged voltage profiles of Cu@g-C_3N_4@Zn symmetric cells at (a) 1 mA cm^{-2}/1 mAh cm^{-2} and (b) 10 mA cm^{-2}/1 mAh cm^{-2}.

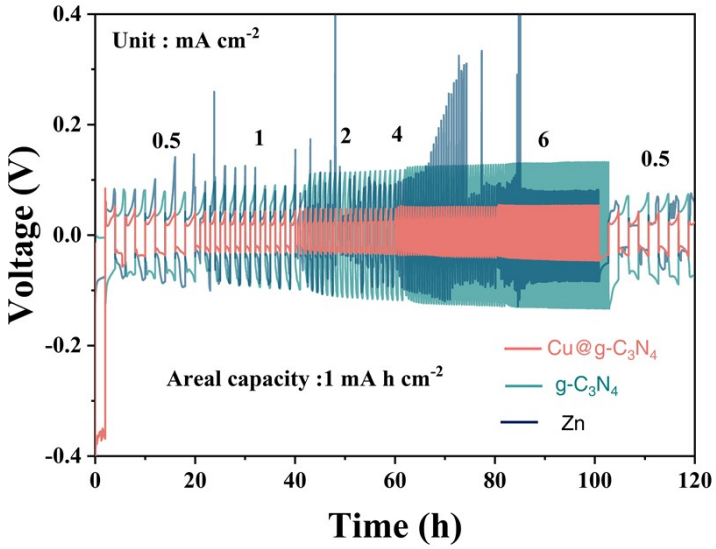

Fig. S11 Rate performance of bare Zn, g-C_3N_4@Zn, and Cu@g-C_3N_4@Zn symmetric cells at current densities from 0.5 to 6 mA cm^{-2} with an areal capacity of 1 mAh cm^{-2}.

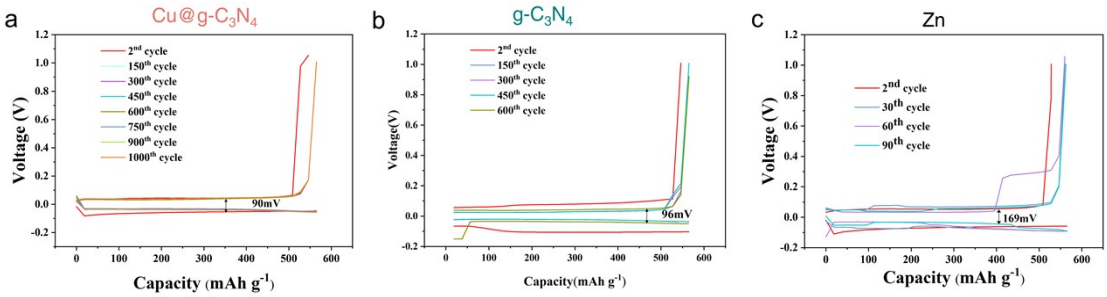

Fig. S12 Voltage–capacity profiles of Zn//Cu cells corresponding to the coulombic-efficiency tests for (a) Cu@g-C_3N_4, (b) g-C_3N_4, and (c) bare Zn interfaces.

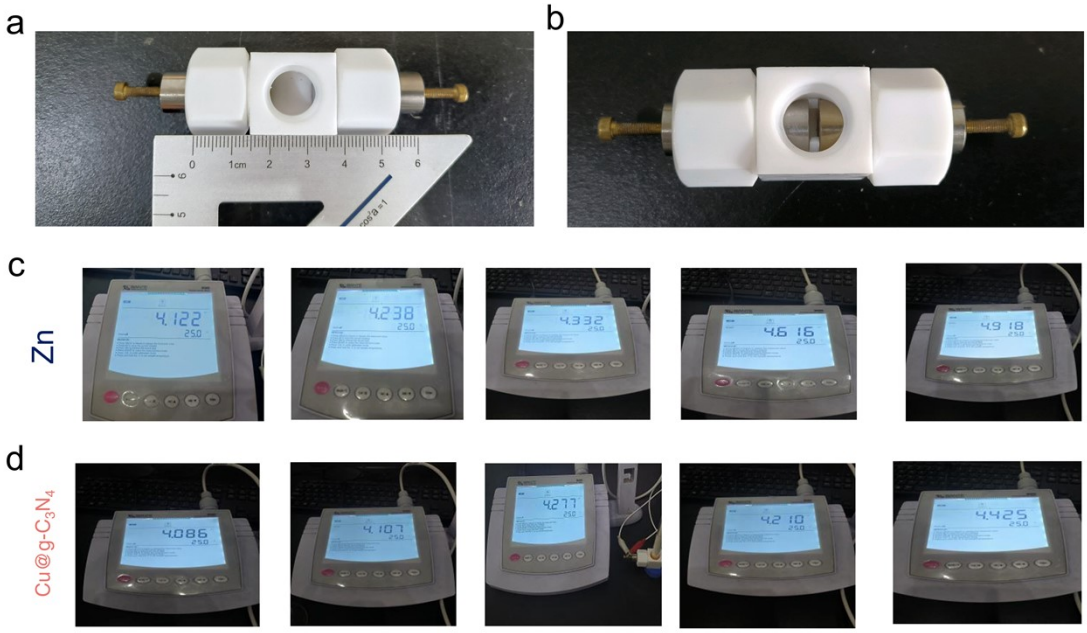

Fig. S13 Photographs of the customized Swagelok-type in-situ pH monitoring device and representative pH readings for bare Zn and Cu@g-C_3N_4@Zn symmetric cells.

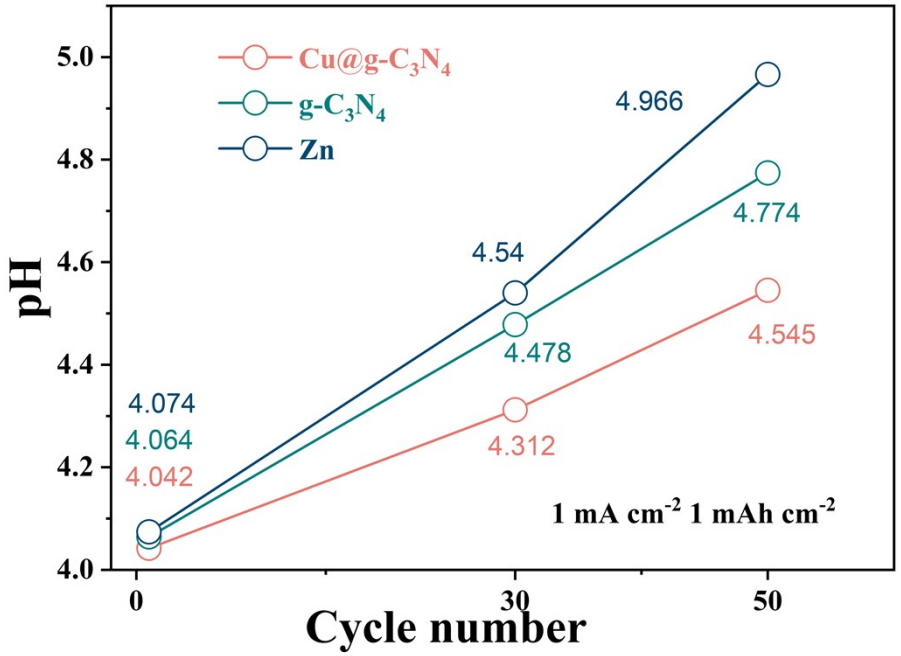

Fig. S14 pH evolution of bare Zn, g-C_3N_4@Zn, and Cu@g-C_3N_4@Zn symmetric cells after 0, 30, and 50 cycles at 1 mA cm^{-2}/1 mAh cm^{-2}.

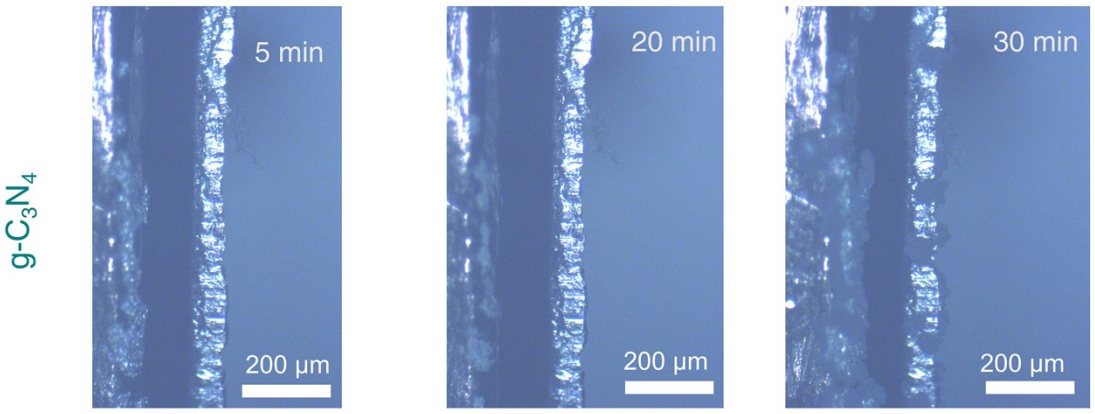

Fig. S15 In-situ optical microscopy images of Zn deposition on g-C_3N_4@Zn after 5, 20, and 30 min of plating. Scale bars: 200 μm.

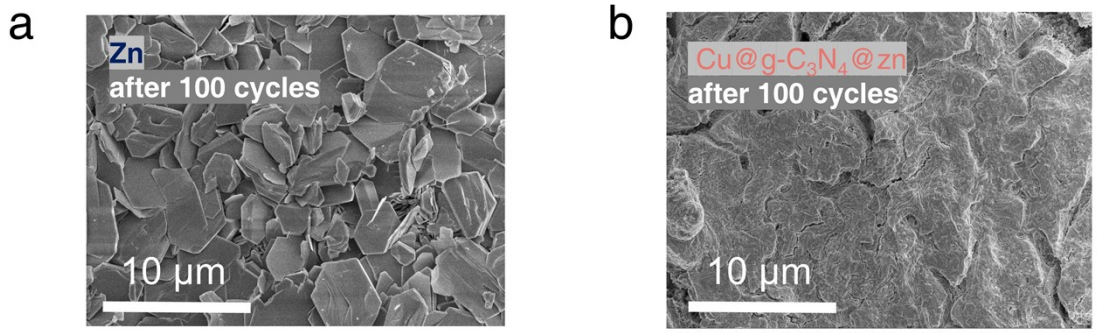

Fig. S16 Post-cycling SEM images of (a) bare Zn and (b) Cu@g-C_3N_4@Zn anodes after 100 cycles at 1 mA cm^{-2}/1 mAh cm^{-2}. Scale bars: 10 μm.

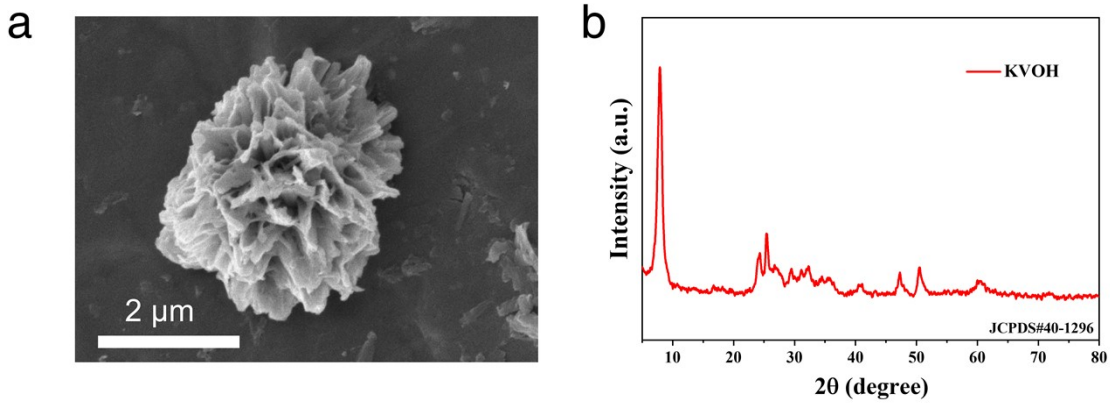

Fig. S17 (a) SEM image and (b) XRD pattern of the KVOH cathode material.

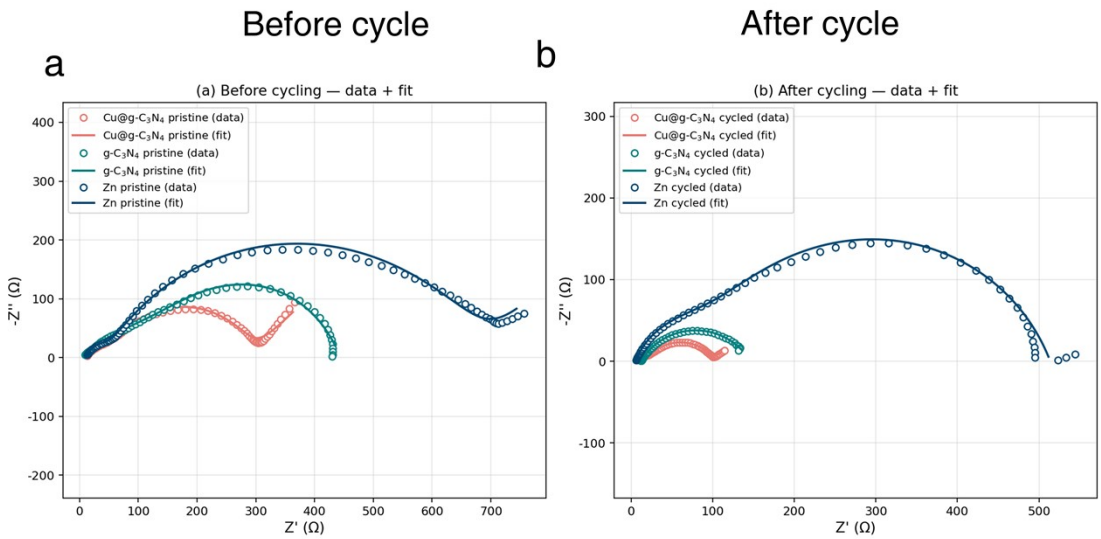

Fig. S18 EIS Nyquist plots and equivalent circuit fitting results of Zn//KVOH full cells (a) before cycling and (b) after cycling.

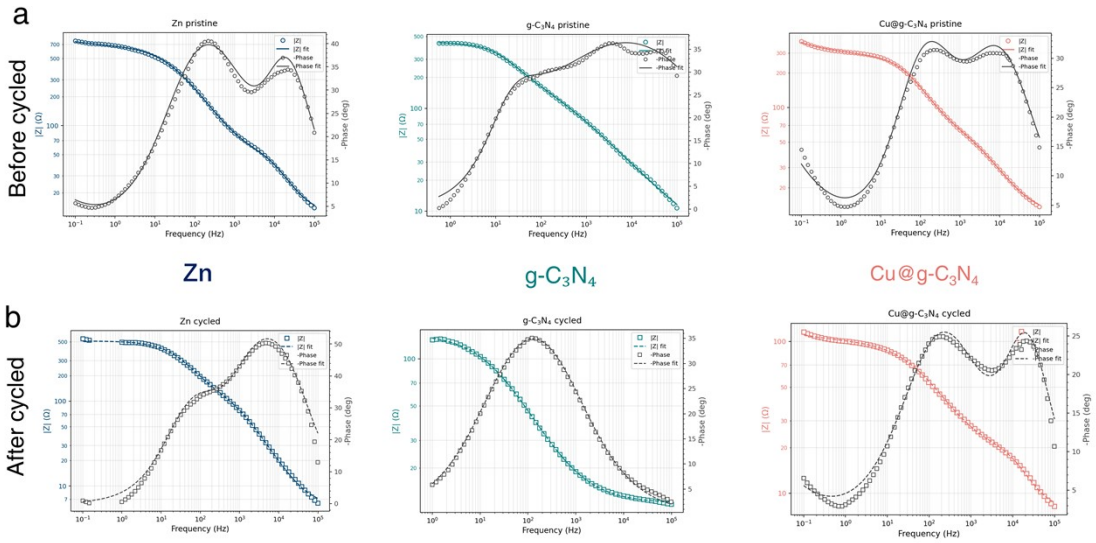

Fig. S19 Bode plots of Zn//KVOH full cells using bare Zn, g-C_3N_4@Zn, and Cu@g-C_3N_4@Zn anodes (a) before and (b) after cycling.

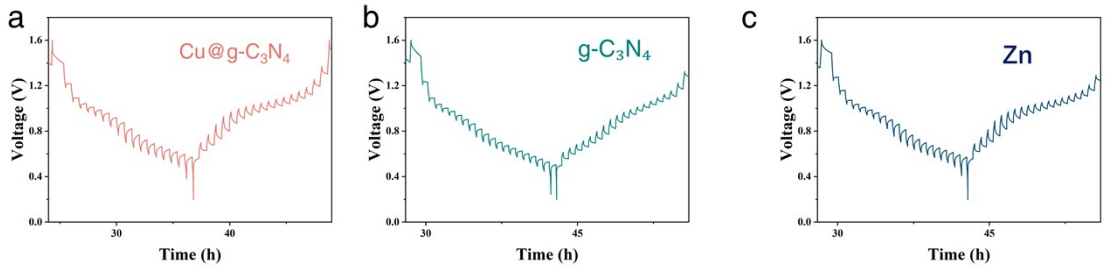

Fig. S20 GITT profiles of Zn//KVOH full cells using (a) Cu@g-C_3N_4@Zn, (b) g-C_3N_4@Zn, and (c) bare Zn anodes.

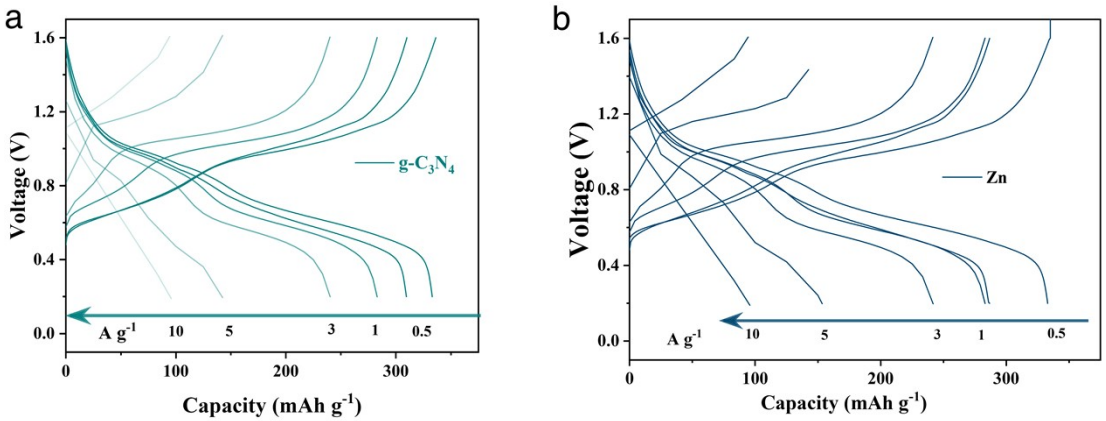

Fig. S21 Charge–discharge profiles of Zn//KVOH full cells using (a) g-C_3N_4@Zn and (b) bare Zn anodes at different current densities.

Table S1 Mass yield of Cu@g-C_3N_4 from thermal polymerization.

Weight of powder plus crucible(g)	Weight of the powder after heating the crucible(g)	Mass of empty crucible(g)	Mass of Cu@g-C_3N_4 produced(g)
40.9797	40.5042	40.4705	0.0337

Table S2 ICP-OES results for Cu content determination in Cu@g-C_3N_4.

Sample Number	Constant volume Vo (mL)	Element	Test solution element concentration C_0 (mg/L)	Sample element content W (%)
Cu@g-C_3N_4	1000	Cu	6.32	4.23%

Table S3 Equivalent-circuit fitting parameters obtained from EIS analysis of Zn//KVOH full cells before and after cycling.

Sample	$R_s = R_0$ (Ω)	$R_f = R_1$ (Ω)	$R_{ct} = R_2$ (Ω)	W σ ($\Omega \cdot s^{-0.5}$)
Zn before cycle	11.78 ± 0.20	29.4 ± 1.3	638.6 ± 6.1	56.2 ± 5.0
Zn cycled	5.63 ± 0.13	88.9 ± 9.8	419.3 ± 16.1	
g-C_3N_4 before cycle	3.60 ± 0.29	222.5 ± 25.1	221.5 ± 25.0	
g-C_3N_4 cycled	11.53 ± 0.06	133.2 ± 0.8	0.5 ± 0.1	
Cu@g-C_3N_4 before cycle	11.16 ± 0.19	46.7 ± 2.5	230.3 ± 3.4	59.9 ± 1.7
Cu@g-C_3N_4 cycled	7.53 ± 0.10	83.5 ± 0.9	10.4 ± 0.5	7.6 ± 0.6

Reference

1 P. E. Blöchl, Projector augmented-wave method. *Phys. Rev. B,* 1994, **50**, 17953-17979.

2 J. P. Perdew, K. Burke, M. Ernzerhof, *Phys. Rev. Lett.,* 1996, **77**, 3865-3868.

3 S. Grimme, J. Antony, S. Ehrlich, H. Krieg, *J. Chem. Phys*., 2010, **132** (15), 154104.